THE JOURNAL OF BIOLOGICAL CHEMISTRY
Vol. 278, No. 33, Issue of August 15, pp. 31202–31209, 2003
Printed in U.S.A.

Phosphatidylinositol Phosphate Kinase Type 1γ and β1-Integrin Cytoplasmic Domain Bind to the Same Region in the Talin FERM Domain*

Received for publication, April 14, 2003
Published, JBC Papers in Press, June 2, 2003, DOI 10.1074/jbc.M303850200

Igor L. Barsukov‡, Andrew Prescot‡, Neil Bate‡, Bipin Patel‡, David N. Floyd‡, Nina Bhanji‡, Clive R. Bagshaw‡, Kresimir Letinic§, Gilbert Di Paolo§, Pietro De Camilli§, Gordon C. K. Roberts‡, and David R. Critchley‡¶

From the ‡Department of Biochemistry, University of Leicester, University Road, Leicester LE1 7RH, United Kingdom and the §Howard Hughes Medical Institute and the Department of Cell Biology, Yale University School of Medicine, New Haven, Connecticut 06510

Talin is an essential component of focal adhesions that couples β-integrin cytodomains to F-actin and provides a scaffold for signaling proteins. Recently, the integrin β_3 cytodomain and phosphatidylinositol phosphate (PIP) kinase type 1γ (a phosphatidylinositol 4,5-bisphosphate-synthesizing enzyme) were shown to bind to the talin FERM domain (subdomain F3). We have characterized the PIP kinase-binding site by NMR using a ^{15}N-labeled talin F2F3 polypeptide. A PIP kinase peptide containing the minimal talin-binding site formed a 1:1 complex with F2F3, causing a substantial number of chemical shift changes. In particular, two of the three Arg residues (Arg^{339} and Arg^{358}), four of eight Ile residues, and one of seven Val residues in F3 were affected. Although a R339A mutation did not affect the exchange kinetics, R358A or R358K mutations markedly weakened binding. The K_d for the interaction determined by Trp fluorescence was 6 μM, and the R358A mutation increased the K_d to 35 μM. Comparison of these results with those of the crystal structure of a β_3-integrin cytodomain talin F2F3 chimera shows that both PIP kinase and integrins bind to the same surface of the talin F3 subdomain. Indeed, binding of talin present in rat brain extracts to a glutathione *S*-transferase integrin β_1-cytodomain polypeptide was inhibited by the PIP kinase peptide. The results suggest that ternary complex formation with a single talin FERM domain is unlikely, although both integrins and PIP kinase may bind simultaneously to the talin anti-parallel dimer.

Integrins are the principal family of receptors mediating cellular interactions with the extracellular matrix (ECM).[1] As such, they support a wide variety of processes that are dependent on cell-ECM interactions including cell proliferation, the suppression of apoptosis, cell migration, and the organization of cells into tissues (1, 2). Integrins are noncovalent αβ-heterodimeric type I transmembrane proteins that are frequently linked to the actomyosin contractile apparatus within the cell via cytoskeletal proteins such as talin (3), filamin (4), and α-actinin (5, 6). Although it is self-evident that such a link is necessary to support integrin-mediated cell migration, these cytoskeletal proteins also recruit, either directly or indirectly, numerous signaling proteins to integrin cytodomains, which regulate cell adhesion, motility, and the signaling pathways that control cell proliferation and apoptosis (7–9). Moreover, expression of an N-terminal fragment of talin, which binds to the β-integrin cytodomain, results in activation of $\alpha_{IIb}\beta_3$-integrin expressed in Chinese hamster ovary cells (3), suggesting that talin directly regulates integrin affinity, possibly by disrupting the interaction between the highly conserved membrane-proximal regions of the αβ-subunit cytodomains (10).

Talin co-localizes with integrins in cell-ECM junctions (focal adhesions; FAs), and microinjection of talin antibodies leads to the disruption of these structures and associated actin stress fibers (11, 12). Down-regulation of talin expression in HeLa cells using antisense RNA slows down the rate of cell spreading and leads to a reduction in the size of FAs (13), and mouse embryonic stem cells in which both copies of the talin gene have been disrupted showed spreading defects and were unable to assemble FAs (14). However, analysis of talin function in mammalian systems is complicated by the recent discovery of a second talin gene (*TLN2*), which we have shown encodes a closely related protein (also 2541 residues, 74% identity) but with a more restricted pattern of expression (15). Nevertheless, mouse embryos with the *TLN1* (−/−) genotype failed to complete gastrulation (16), probably because of a failure of mesoderm migration, and in *Drosophila*, deletion of the single talin gene gives rise to phenotypes very similar to integrin null alleles (17).

The known biochemical properties of talin are also consistent with a role in linking integrins to F-actin. It is a large (270 kDa) flexible rod-shaped (600 nm) (18) actin-cross-linking protein (19) 2541 residues in length (20, 21). The globular talin head contains a region (residues 86–410) homologous to the N-terminal FERM domain of the band 4.1, ezrin, radixin, moesin family of cytoskeletal proteins (20, 22), and has binding sites for the cytoplasmic domains of β_{1A}, β_{1D} (23), and β_3 (24) integrins (K_d = ~100 nM) (25) as well as the C-type lectin layilin (26), the protein-tyrosine kinase FAK (26), and F-actin (21). The talin rod, which is responsible for the assembly of the talin anti-parallel dimer (27), contains a highly conserved C-termi-

* This work was supported by Wellcome Trust grants (to D. R. C. and C. R. B.) and a Biotechnology and Biological Sciences Research Council (BBSRC) SMART initiative grant (to D. R. C., I. L. B., and G. C. K. R.). The costs of publication of this article were defrayed in part by the payment of page charges. This article must therefore be hereby marked "*advertisement*" in accordance with 18 U.S.C. Section 1734 solely to indicate this fact.

¶ To whom correspondence should be addressed: Dept. of Biochemistry, University of Leicester, University Rd., Leicester LE1 7RH, UK. Tel.: 116-252-3477; Fax: 116-252-3369; E-mail: drc@le.ac.uk.

[1] The abbreviations used are: ECM, extracellular matrix; FA, focal adhesion; PIP, phosphatidylinositol phosphate; PIP2, phosphatidylinositol 4,5-bisphosphate; GST, glutathione *S*-transferase; HSQC, heteronuclear single-quantum correlation.

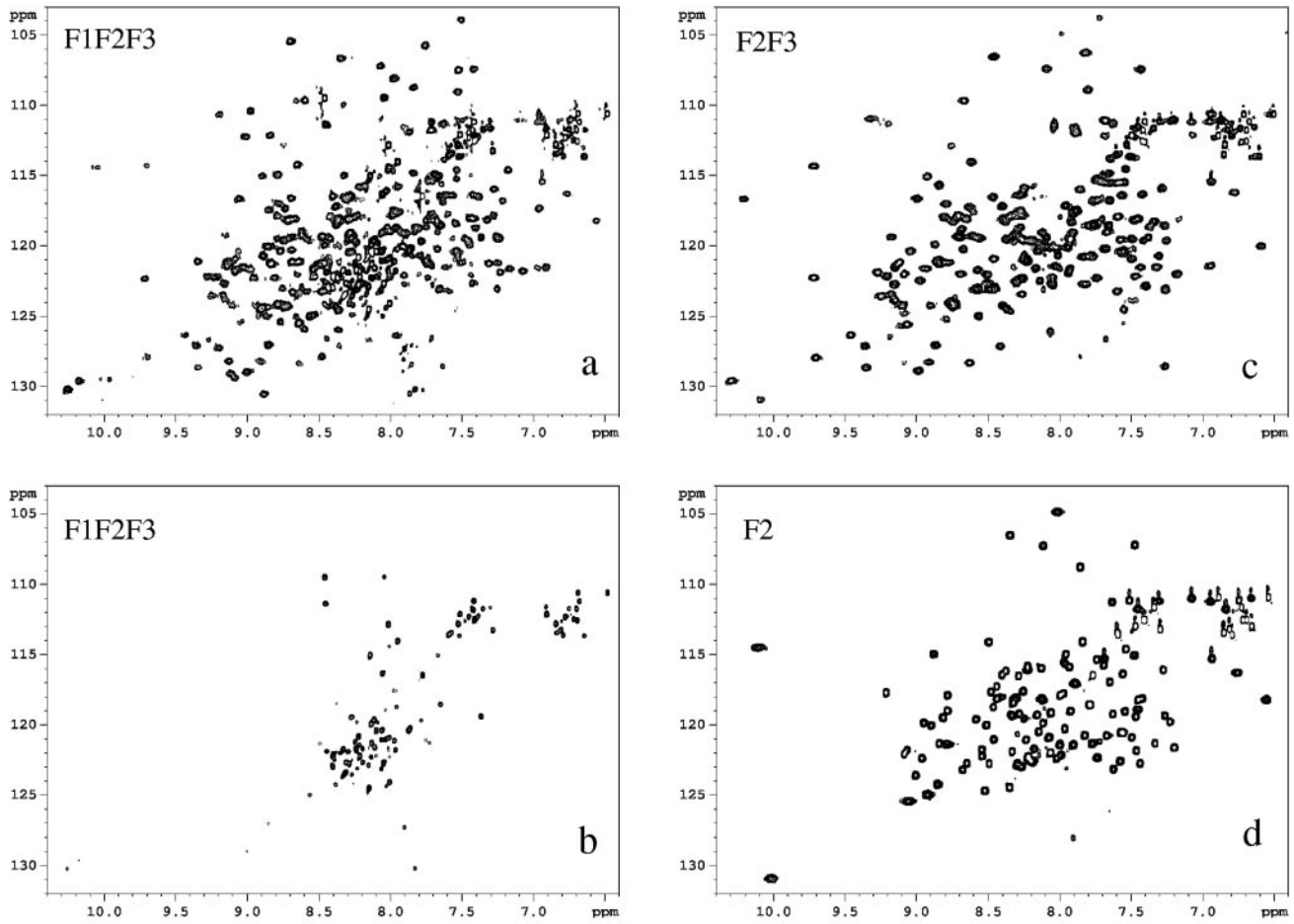

FIG. 1. **^{15}N,^{1}H-HSQC spectra of uniformly ^{15}N-labeled talin polypeptides.** *a* and *b*, F1F2F3. *c*, F2F3. *d*, F2. The spectrum of F1F2F3 is shown with low (*a*) and high (*b*) contour levels to highlight sharp intense cross-peaks.

nal actin-binding site (residues 2345–2541) (21, 28), which probably accounts for the actin-cross-linking activity of talin. It also contains a second lower affinity integrin-binding site (residues 1984–2541) (25, 29), and three binding sites for the cytoskeletal protein vinculin (30), which in turn has multiple binding partners.

The recently determined crystal structure of the talin FERM domain (subdomains F2/F3) fused to part of the β_3-integrin cytodomain shows that the F3 subdomain resembles a phosphotyrosine-binding domain (31) that typically recognize NPXpY motifs in proteins. Indeed, the membrane-proximal NPXY motif in the integrin cytoplasmic domain is essential for talin binding (3). Integrin binding occurs through a mainly hydrophobic area in the talin F3 subdomain centered on the β_5-strand and involving residues of the β_6-strand, the C-terminal half of helix 5, and the β_4-β_5 loop. Integrin residues Trp^{739}–Tyr^{747} all make direct contact with talin with the exception of Asn^{743}. As expected, mutation of talin residues predicted to be involved in integrin binding (Arg^{358}, Trp^{359}, and Ile^{396} to alanine) abolishes or markedly reduced binding of a GST-talin F2/F3 polypeptide to a His-tagged integrin β_3-subunit cytodomain peptide immobilized on nickel-coated beads.

Interestingly, the talin F3 subdomain has also recently been shown to bind to the C-terminal 28 residues of an alternatively spliced isoform of PIP4′P-5′ kinase type 1γ, which is localized in FAs (32, 33). The talin/PIP kinase interaction is adhesion-dependent (33), and activates the PIP kinase (32), which is then reported to drive talin from a cytoplasmic pool to the plasma membrane and to facilitate its incorporation into FAs (33). A PIP kinase-dead mutant can support the translocation of talin to the membrane but disrupts talin and FAK localization to FAs (33). This suggests a model in which cell/ECM interaction somehow triggers the assembly of a talin/PIP kinase type 1γ complex that translocates to the plasma membrane, resulting in a highly localized increase in phosphatidylinositol 4,5-bisphosphate (PIP2) concentration. The integrin-binding sites in talin are masked and have been shown to be activated by PIP2 *in vitro* (34). Talin activated in this way might then bind to and in turn activate integrins, rendering them competent to engage the ECM. Such an ECM/integrin/talin complex might then interact with F-actin leading to FA assembly and be further stabilized by the recruitment of vinculin (35), which also binds to and is activated by PIP2 (36, 37). Such a model is consistent with the fact that cell adhesion to fibronectin increases PIP2 levels (38, 39) and that PIP2 increases the strength of the adhesion energy between the membrane and the actin cytoskeleton (40).

One of the questions raised by this study is whether an ECM/integrin/talin complex might also include PIP kinase or whether both integrins and PIP kinase compete for binding to the same pocket on the talin F3 subdomain. To address this question, we have used NMR and fluorescence to assay the interaction between a talin F2/F3 subdomain polypeptide and a synthetic PIP kinase peptide containing the minimal talin-binding sequence. The results show that Arg^{358} in the talin F3 subdomain is involved in binding both the PIP kinase type 1γ and the β-integrin. Moreover, the ability of the GST-β_1-integrin cytoplasmic domain to bind talin is inhibited by a PIP kinase type 1γ peptide.

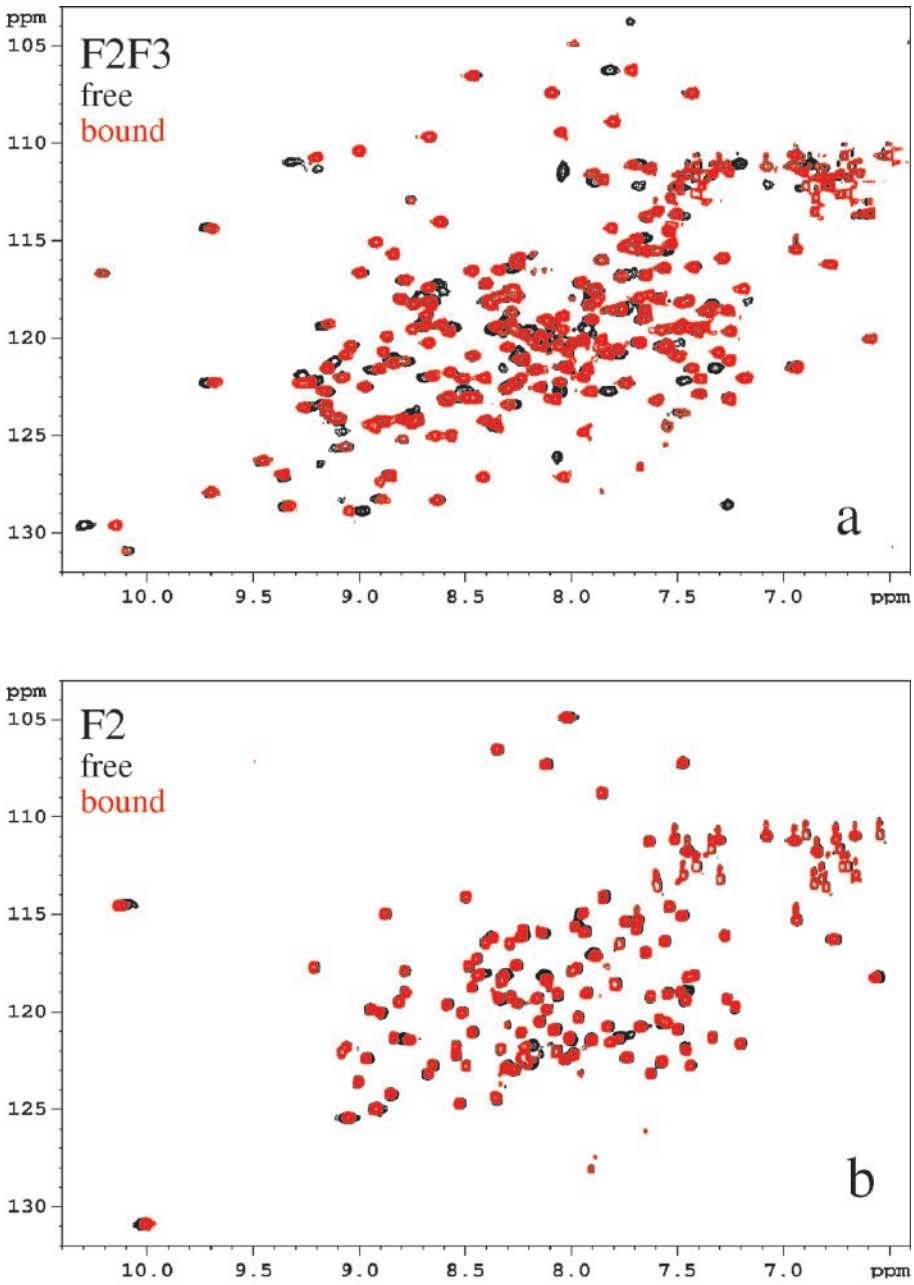

FIG. 2. **Comparison of the $^{15}N,^{1}H$-HSQC spectra of talin polypeptides plus or minus the PIP kinase peptide.** F2F3 (*a*) and F2 (*b*) in the free form (*black*) and in the presence of PIP kinase peptide (*red*) are shown.

MATERIALS AND METHODS

Protein Expression and Purification—All of the talin constructs were amplified by PCR from a mouse cDNA (20) and cloned into the *Nde*I and *Bam*HI sites of the pET15b prokaryotic expression vector. Uniformly ^{15}N-labeled His-tagged proteins were expressed at 37 °C as described by Marley *et al.* (41) or were selectively labeled with ^{15}N-Ile or ^{15}N-Val (Cambridge Isotope Laboratories, Inc). The proteins were purified using a nickel affinity column and cleaved with thrombin following standard protocols (Amersham Biosciences). The reaction was stopped by the addition of 1 mM phenylmethylsulfonyl fluoride, and the protein was further purified using a SP Sepharose cation exchange column (Amersham Biosciences) followed by gel filtration using a Superdex 75 column (Amersham Biosciences) in 20 mM sodium phosphate, 150 mM NaCl, pH 6.5 (NMR buffer). All of the proteins were stable and could be concentrated to ~1 mM without any significant effect on the quality of the NMR spectra.

Binding of Talin Polypeptides to PIP Kinase Analyzed by NMR and Fluorescence—A PIP kinase peptide containing the minimal talin-binding site (32) (underlined) ^{642}TDERSWVYSPLHYSAQA^{658} was synthesized, and the sequence confirmed by mass spectroscopy. Purity of >85% was estimated by high pressure liquid chromatography. The protein and peptide concentrations were determined from the UV absorbance at 280 nm. Binding of the PIP kinase peptide (10 mM stock solution in NMR buffer) to talin polypeptides was followed using one-dimensional ^{1}H and two-dimensional $^{1}H,^{15}N$-HSQC spectra acquired at 600 MHz on a Bruker DRX600 spectrometer at 25 °C. The spectra were processed and analyzed using XWINNMR 3.1 software (Bruker) and were referenced to the external DSS standard at 0.000 ppm.

Fluorescence spectra were recorded using an SLM 48000 spectrofluorimeter or a Varian Eclipse spectrofluorimeter at 20 °C and were corrected for background emission. Stopped flow records were captured using an Applied Photophysics SX18MV instrument with excitation at 297 nm and the emission collected through WG320 and UG11 filters as described previously (42). The data were fitted to single exponentials to extract an observed rate constant $k_{obs} = k_{+1}[\text{PIP kinase}] + k_{-1}$, where k_{+1} and k_{-1} represent the association and the dissociation rate constant, respectively. Single exponential fits were satisfactory at low concentrations of the PIP kinase peptide, despite approaching second order conditions caused by the dominating contribution from k_{-1}.

Affinity Chromatography of Talin from Rat Brain Extract—The affinity chromatography experiments were performed as previously described (32). Briefly, 2-mg rat brain Triton X-100 extracts were affinity-purified on Sepharose 4B columns containing 200 μg of GST or GST fusions of the 28-amino acid C-terminal tail of human PIP kinase Iγ 90 (641–668) as well as of the integrin β_1 cytodomain (43) in 25 mM Hepes, pH 7.4, 150 mM KCl, 1 mM EDTA, and 1% Triton X-100 supplemented

with a mixture of protease inhibitors. Following four washes with the same buffer, affinity-purified material was eluted in sample buffer and processed for SDS-PAGE and immunoblotting or Coomassie Blue staining. In competition experiments, the brain extracts were preincubated for 30 min at 4 °C with a PIP kinase synthetic peptide containing the minimal talin-binding site (32) (underlined) ^{643}DERSWVYSPLHYS^{655} and a control peptide W647A,P651A at various concentrations.

RESULTS AND DISCUSSION

Analysis of the Talin FERM Domain by NMR—Comparison of ^{15}N-HSQC spectra of the complete talin FERM domain (F1F2F3; residues 86–410), the F2F3 subdomains (residues 196–400), and the F2 subdomain alone (residues 196–309) is presented in Fig. 1. The notable feature of the F1F2F3 spectra is the presence of ~30 relatively sharp and intense cross-peaks, indicative of an unstructured and highly mobile region (Fig. 1, *a* and *b*). This region is localized to the F1 subdomain because the spectra of F2F3 (Fig. 1*c*) or F2 (Fig. 1*d*) alone do not have this feature and probably represents the insert predicted to exist in F1 based on sequence alignments (22). The absence of extensive unstructured regions in the F2F3 and F2 polypeptides demonstrates that fragments of the FERM domain expressed separately retain a globular structure that includes the N- and C-terminal regions. Moreover, superimposition of the spectra of the F2 and F2F3 polypeptides with that of the complete FERM domain reveals that the majority of the cross-peaks have the same position, indicating that the smaller polypeptides adopt the native structure. However, some cross-peaks of the smaller polypeptides do not have a corresponding cross-peak at the same position in the F1F2F3 polypeptide, indicating direct contact between the individual subdomains. All of these observations are entirely consistent with the known structural characteristics of FERM domains, which consist of three globular subdomains connected by short linkers (22).

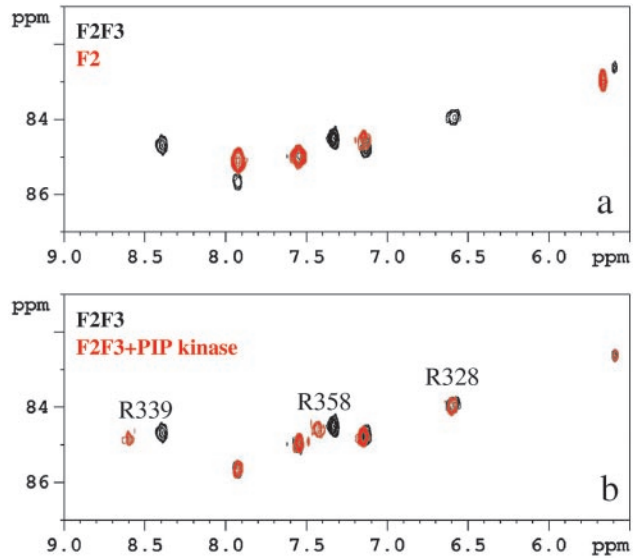

FIG. 3. **Comparison of the Arg side chain ^{15}N,^{1}H-HSQC resonances of talin F2F3 and F2 polypeptides plus or minus the PIP kinase peptide.** *a*, regions of the ^{15}N,^{1}H-HSQC spectra corresponding to the Arg side chain resonances of talin polypeptides F2F3 (*black*) and F2 (*red*) in the free form; *b*, F2F3 fragment in the free form (*black*) and in the presence of equimolar amount of PIP kinase peptide (*red*). Assignments of Arg residues from the F3 fragment obtained using site-directed mutagenesis are indicated in *b*.

Analysis of Binding of the Talin FERM Domain to PIP Kinase Type 1γ by NMR—Addition of the PIP kinase peptide ^{642}TDERSWVYSPLHYSAQA^{658} resulted in significant changes in the ^{15}N-HSQC spectra of all three uniformly labeled talin polypeptides. In the case of F2F3 (Fig. 2*a*) and F1F2F3 (data not shown), the exchange between the free and the bound states was slow on the NMR time scale as shown by the appearance of new cross-peaks in the ^{15}N-HSQC spectra upon the addition of peptide. The intensity of these peaks increased with increasing peptide concentration and reached a maximum at a 1:1 molar ratio. In parallel, a similar number of resonances decreased in intensity and disappeared at a 1:1 molar ratio. Further addition of peptide did not produce any changes in the ^{15}N-HSQC spectrum, and sharp resonances corresponding to the signals of the free peptide appeared in the proton spectrum. The PIP kinase peptide also caused specific changes in the F2 spectra (Fig. 2*b*), but the number of affected resonances and the extent of the changes were substantially smaller than with the

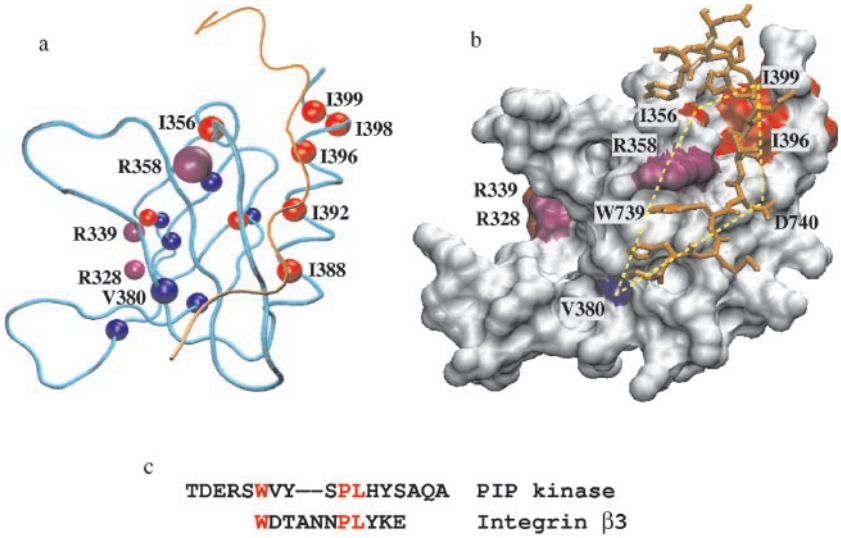

FIG. 4. **The integrin-binding surface in the talin F3 subdomain.** *a*, the distribution of Arg (*magenta*), Ile (*red*), and Val (*blue*) in the structure of the talin F3 subdomain determined by x-ray crystallography (31). The *balls* are centered on the backbone nitrogen atoms for Ile and Val and on the side chain Nε for Arg. The position of part of the integrin cytodomain as determined by x-ray crystallography of an integrin cytodomain/talin F2F3 chimera (31) is shown as an *orange tube*. *b*, surface representation of the talin F3 subdomain showing the exposure to the solvent of the Arg (*magenta*), Ile (*red*), and Val (*blue*) side chains. The integrin cytodomain is shown in *orange*, and the positions of Trp^{739} and Asp^{740} are indicated. The *yellow dotted line* marks the surface expected to be in contact with PIP kinase from the chemical shift perturbations and studies with the talin mutants. *c*, sequence alignment between the integrin cytodomain peptide used in the integrin/talin chimera (31) and the PIP kinase peptide used in the current study as suggested in Ref. 48.

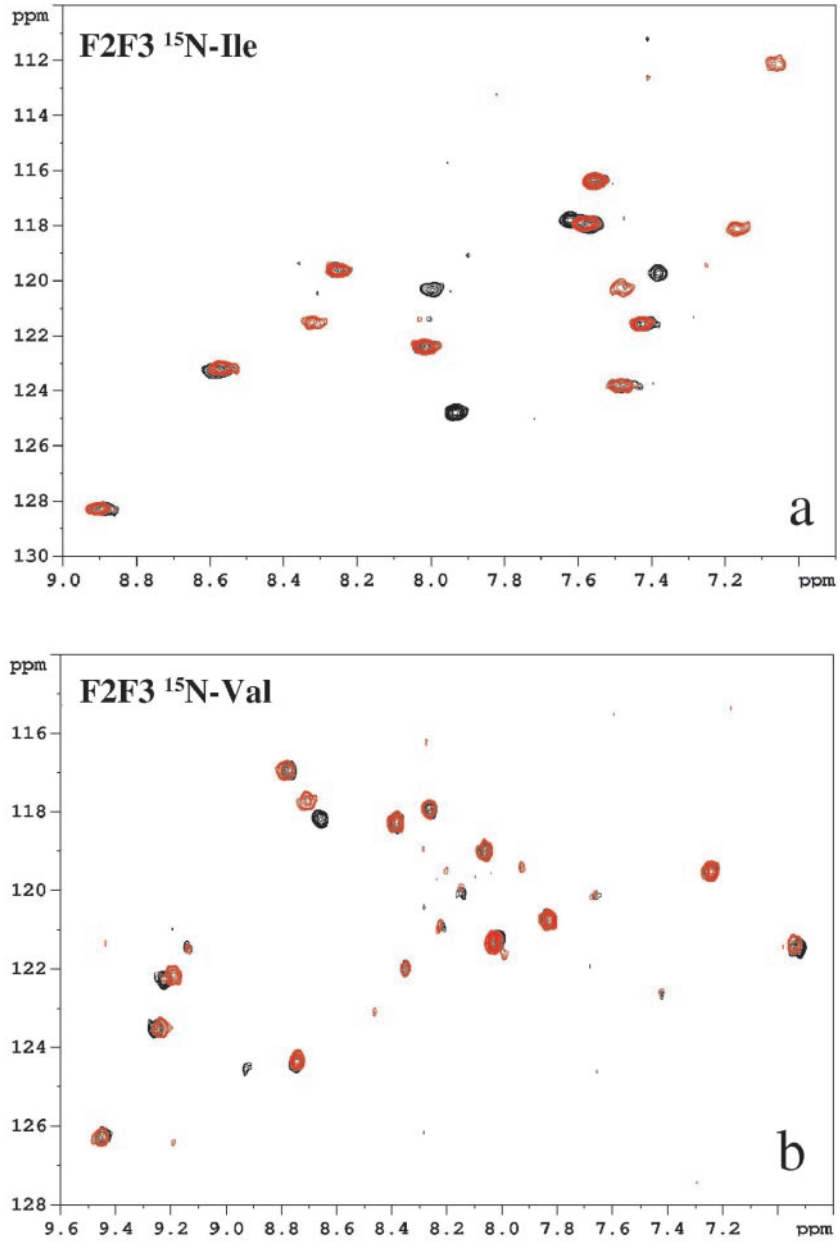

FIG. 5. **Comparison of the Ile and Val side chain $^{15}N,^{15}H$-HSQC resonances of the talin F2F3 plus or minus the PIP kinase peptide.** $^{15}N,^{1}H$-HSQC spectra of the talin F2F3 polypeptide selectively ^{15}N-labeled at Ile (*a*) or Val (*b*) residues in the free form (*black*) and in the presence of equimolar amount of PIP kinase peptide (*red*) are shown.

F2F3 polypeptide. Moreover, titration of F2 with peptide lead to a gradual shift of the affected cross-peaks, corresponding to fast exchange on the NMR time scale. The data demonstrate that the interaction of the PIP kinase peptide with the F1F2F3 and F2F3 subdomains is much stronger than that with the F2 subdomain and that the number of residues involved in binding is much larger in the former case. This suggests that the F3 subdomain contains the main binding site for PIP kinase. This result is in complete agreement with the data of Di Paolo *et al.* (32), who mapped the PIP kinase-binding site to the talin F3 subdomain using pull-down assays. At the same time the specific changes observed in the F2 spectra upon peptide binding may indicate a significant contribution from this domain to the binding interaction.

Characterization of the PIP Kinase-binding Site in the Talin F3 Subdomain—The location of the PIP kinase-binding site within F3 was deduced from analysis of the peptide-induced perturbations in the ^{15}N-HSQC spectra of the F2F3 subdomain. Initially, we used the well resolved cross-peaks corresponding to the Arg side chains. Seven cross-peaks were observed for F2F3 and four for F2 (Fig. 3), in agreement with the four Arg residues in F2 and three in F3. The cross-peaks of the three Arg residues from the F3 subdomain are easily identified from spectra comparisons, and addition of the PIP kinase peptide affects the position of two of these cross-peaks (Fig. 3*b*). None of the F2 cross-peaks are affected (data not shown). We assigned the F3 Arg side chain resonances to specific residues using site-directed mutagenesis. Single-residue substitutions at R328A, R339A, and R358A (or R358K) each led to the disappearance of a single cross-peak in the ^{15}N-HSQC spectra, whereas the other Arg side chain resonances were observed in positions close to those of the wild type. The resonance assignments derived in this way show that PIP kinase binding affects the side chains of Arg^{339} and Arg^{358}. Titration experiments demonstrate different roles for these residues in PIP kinase binding. For the R339A mutant, slow exchange on the NMR time scale was observed, similar to that of the wild type. For the R358A and R358K mutants, the exchange between the free and the bound forms was on the intermediate NMR time scale, as shown by the extensive broadening of a large number of resonances in the F2F3 spectra at a 1:0.5 molar ratio of F2F3/peptide. This indicates a direct involvement of R358 in peptide

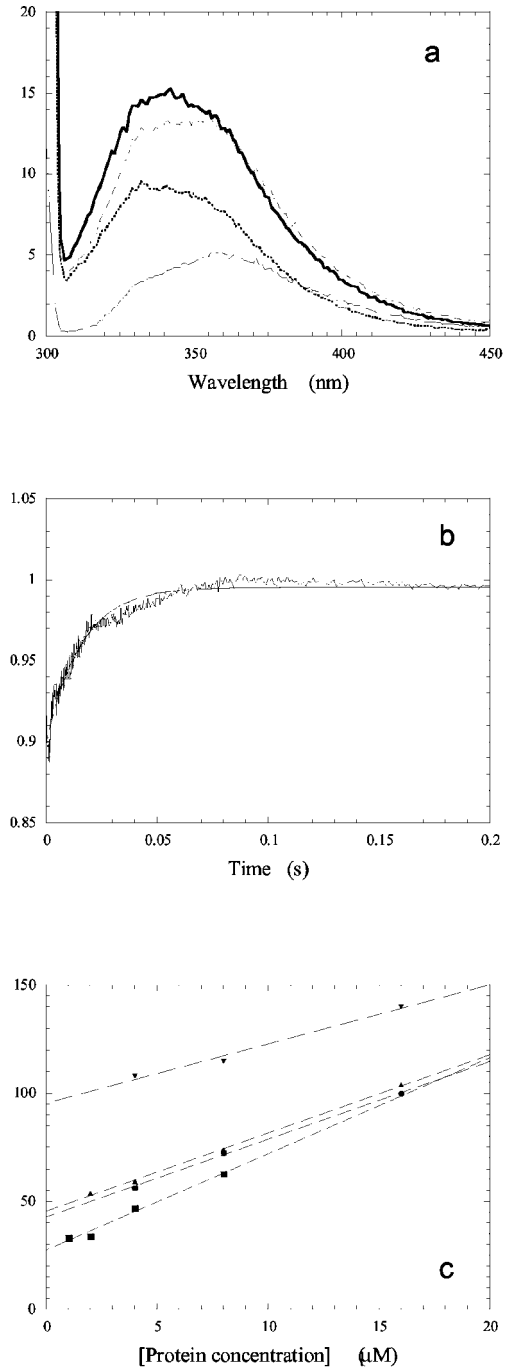

FIG. 6. **Binding of the PIP kinase peptide to talin F2F3 assayed by fluorescence.** *a*, emission spectra of 4 μM PIP kinase (*solid line*), 4 μM talin F2.F3 (*dotted line*), the computed sum (*dashed line*), and experimental mixture (*bold line*) on excitation at 297 nm. Note the 10% enhancement in fluorescence at 340 nm but the loss of the shoulder attributed to free PIP kinase above 380 nm in the mixture. *b*, stopped flow record of Trp fluorescence on mixing 8 μM PIP kinase with 8 μM talin F2.F3 (reaction chamber concentrations) with a superposed fit to an exponential with a rate constant k_{obs} = 63 s^{-1}. *c*, plot of observed rate constant against protein concentration from stopped flow transients as exemplified in *b* for PIP kinase binding to wild type talin F2F3 (■), R339A talin F2F3 (●), R328A talin F2F3 (▲), and R358A talin F2F3 (▼). These data are analyzed in Table I. All of the experiments were carried out in 100 mM NaCl, 20 mM phosphate buffer at pH 6.5 and 20 °C.

binding, whereas the lack of affect of the R339A mutation suggests that this residue is located in the vicinity of the binding site but is not in direct contact.

Further refinement of the PIP kinase-binding site was

TABLE I
Kinetic parameters for the interaction between the PIP kinase peptide and talin F2F3 assayed by fluorescence stopped flow

F2F3 polypeptide	k_{off}	k_{on}	k_{off}/k_{on}
	s^{-1}	$\mu M^{-1}\ s^{-1}$	μM
Wild type	27	4.4	6
R328A	45	3.6	12
R339A	42	3.6	12
R358A	95	2.7	35

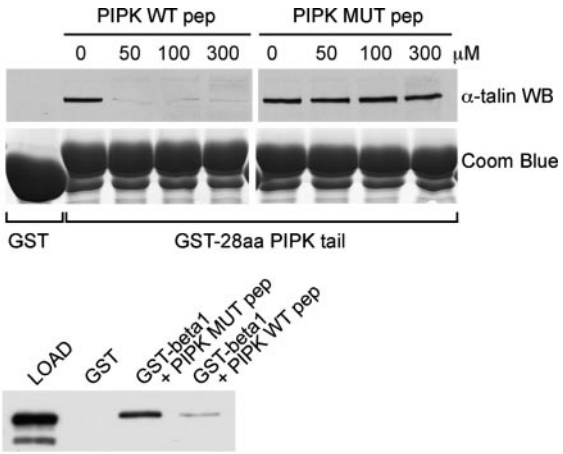

FIG. 7. **A PIP kinase peptide competes the binding of talin to immobilized integrin β_1 cytodomain.** *Top panel*, Western blot showing the affinity purification of talin from rat brain detergent extract using a GST fusion of the 28-amino acid C-terminal tail of PIP Kinase type Iγ 90. A short peptide containing the talin-binding peptide WVYSPL (*PIPK WT pep*) competes and abolishes this interaction at concentrations as low as 50 μM. A control peptide in which the Trp and Pro residues have been substituted with an alanine (*PIPK MUT pep*) does not compete this interaction at concentration as high as 300 μM. *Bottom panel*, Western blot showing the affinity purification of talin from brain extract using a GST fusion of the integrin β_1 cytodomain as a bait. The wild type PIP kinase peptide used at 50 μM efficiently competes the talin-integrin interaction, unlike the mutant peptide.

achieved through the use of residue-specific ^{15}N labeling. The distribution of Ile and Val residues in the F3 crystal structure (31) is shown in Fig. 4*a*. The majority of Ile residues are located in the long C-terminal helix H5 in the vicinity of Arg^{358} but almost on the opposite face of the molecule from Arg^{339}. In contrast, most of Val residues are located in the vicinity of Arg^{328} and Arg^{339} distant from helix H5. We observed very large chemical shift changes of the backbone HN groups of four of eight Ile, and a much smaller change in the position of one of the seven Val cross-peaks (Fig. 5), clearly indicating the involvement of helix H5 in the interaction with the peptide. This helix contains five Ile residues with Ile^{392}, Ile^{396}, and Ile^{399} being the most likely to contribute to binding as their side chains are exposed. Additionally, the side chain of Ile^{356} is directed toward the helix H5 and could also be involved. The only Val residue that has an exposed side chain on the same surface is Val^{380}, which agrees with the smaller effect of peptide binding on the Val resonances.

Analysis of Talin FERM Domain/PIP Kinase Peptide Binding by Fluorescence—The presence of a Trp residue in the PIP kinase peptide allowed us to use fluorescence to monitor the protein/peptide interactions. The emission maximum of the free PIP kinase peptide was 365 nm, typical of a Trp ring in an aqueous environment, whereas the Trp in the talin fragments emitted at 338 nm indicative of buried residues. In the presence of the F2F3 fragment, the PIP kinase Trp emission shifted to a shorter wavelength, and the observed fluorescence was enhanced at 340 nm by 10% compared with the computed sum

of the free talin and PIP kinase emission (Fig. 6*a*). The time course of the fluorescence enhancement upon binding was resolved by the stopped flow technique (Fig. 6*b*), allowing evaluation of the association and dissociation rate constants for the binding process. Kinetic parameters were evaluated from stopped flow fluorescence experiments performed on the wild type F2F3 polypeptide, as well as the Arg mutants and are summarized in Table I. The R358K and R358A mutants show a large reduction in binding affinity. The increase in k_{off} for the Arg^{358} mutants would be predicted to alter the exchange characteristics from slow to intermediate on the NMR time scale. As can be seen in Fig. 5*a*, the chemical shift difference between the free and the bound states are 0.2–0.4 ppm for ^1H, corresponding to 120–240 Hz at 600 MHz. These values are much larger than k_{off} for the wild type F2F3 polypeptide, compatible with slow exchange but are comparable with the k_{off} for the Arg^{358} mutants, consistent with intermediate exchange and the strong exchange broadening observed.

A Model of the Talin F3 Subdomain/PIP Kinase Interaction—The observed NMR spectral changes in the talin F3 subdomain upon PIP kinase binding and the effect of F3 mutations on the interaction maps the minimal PIP kinase-binding site in F3 to the area marked in *yellow* in Fig. 4*b*. This includes the surface formed by the β_5 strand and the helix H5. The same surface had been identified as the main binding area for the integrin cytodomain by crystallographic studies on a talin F2F3-integrin chimera (31). According to this structure, the side chain of the Trp residue present in the integrin cytodomain at position −8 relative to the NP*X*Y motif serves as one of the main determinants of the interaction. This side chain is slotted into a hydrophobic pocket in the talin F3 subdomain formed by the side chains of Arg^{358}, Ala^{360}, and Tyr^{377}. The guanidinium group of Arg^{358} forms a hydrogen bond with the hydroxyl group of Tyr^{377} and a salt bridge to Asp^{369} that leads to the stabilization of the pocket. Mutation of Arg^{358} to Ala markedly reduces binding of talin F2F3 to the β_3-integrin cytodomain in pull-down assays (31). The integrin polypeptide chain runs along the hydrophilic stretch of the F3 surface formed by the β_5 strand and the helix H5 (31) (Fig. 4) in the proximity of Ile^{392}, Ile^{396}, and Ile^{398}. The turn in the C-terminal part of the integrin cytodomain at Pro^{745} brings the chain into contact with Ile^{356} in talin F3. The linker region at the N-terminal part of the integrin sequence is in proximity with Val^{380}.

Overall, the mode of binding of the integrin peptide fits well with our experimental data on talin/PIP kinase interaction. Thus, R358A or R358K mutations in F3 substantially increase the K_d value for the PIP kinase peptide. The similarities between integrin and PIP kinase binding also extend to the fact that both also interact weakly with the F2 subdomain (3). Alignment of the PIP kinase peptide with integrin sequences show that substitutions of integrin residues Asp^{740} and Thr^{741} to Val and Tyr, respectively, in PIP kinase (Fig. 4*c*) make it more suitable for binding to the hydrophobic stretch present on the talin F3 surface. Stronger binding of PIP kinase is therefore predicted. Indeed, we failed to detect any binding of a synthetic integrin β_3 subunit cytodomain peptide EERARAKWDTAN<u>NPLY</u>KEATS (the NP*X*Y motif is underlined) to talin F2F3 either by NMR or by fluorescence. This suggests that although the WDTAN<u>NPLY</u> region is required, it is not sufficient for integrin binding, and that other regions of the integrin cytodomain must be involved as reported previously (29). Consistent with this, talin binding results in NMR chemical shift changes in the membrane-proximal region of the integrin cytodomain (44).

Binding of Talin to GST β_1-Integrin Cytoplasmic Domain Is Inhibited by a PIP Kinase Type 1γ Peptide—To confirm that the PIP kinase type 1γ90 isoform and the integrin β-cytodomain binds to the same or an overlapping site in the talin F3 subdomain, we sought to establish whether a PIP kinase peptide containing a minimal talin-binding site could inhibit the integrin/talin interaction. The results in Fig. 7 (*top panel*) show that talin present in a rat brain detergent extract binds specifically to a GST-PIP kinase fusion protein and that a short PIP kinase peptide containing the sequence WVYSPL competes out binding, whereas a peptide in which the Trp/Pro residues were mutated to alanine had no such activity. These PIP kinase peptides were then examined for their ability to inhibit binding of talin to a GST integrin β_1-cytodomain construct. Talin present in the brain extract bound specifically to the GST β_1-cytodomain, and binding was significantly inhibited by the wild type PIP kinase peptide but not that containing the Trp/Pro to alanine substitution (Fig. 7, *bottom panel*). These results provide compelling evidence that the integrin β_1-cytodomain binds to the talin FERM domain at or close to the same site as PIP kinase.

Previous studies have shown that an adhesion-dependent interaction between talin and PIP kinase results in activation of the kinase and translocation of the complex to the plasma membrane (33). Here, localized synthesis of PIP2 might activate the integrin-binding sites in talin (34) and facilitate the assembly of integrin/talin complexes. However, because integrins and PIP kinase both bind to the same region in the talin FERM domain, the question arises of whether a mechanism is required to facilitate transfer of talin from PIP kinase to integrins. Tyrosine phosphorylation of PIP kinase by FAK is reported to increase the affinity of the interaction between talin and PIP kinase (33), and a tyrosine phosphatase such as Shp2, which regulates FA turnover (45), may be required to weaken the link. Alternatively, synthesis and subsequent binding of PIP2 to the talin head (46) may simultaneously increase its affinity for integrins and decrease that for PIP kinase. However, because talin is reported to contain a second integrin-binding site in the rod region (25, 29) and is also an antiparallel dimer (47), it is possible that both PIP kinase and integrins may co-exist within talin complexes, and indeed PIP kinase type 1γ co-localizes with talin in FAs (32, 33).

Acknowledgments—We are grateful to Dr. Jari Ylanne (University of Oulu, Oulu, Finland) for the kind gift of GST-integrin β_1 tail construct, to John Keyte (Biopolymer Synthesis and Analysis Unit, School of Biochemical Sciences, Faculty of Medicine and Health Sciences, University of Nottingham) for peptide synthesis, and to Prof. Robert C. Liddington (Burnham Institute, La Jolla, CA) for the PDB file of the talin F2F3 crystal structure in advance of publication.

REFERENCES

1. Hynes, R. O. (2002) *Cell* **110,** 673–687
2. Hemler, M. E. (1999) in *Guidebook to the Extracellular Matrix, Anchor and Adhesion Proteins* (Kreis, T., and Vale, R., eds) 2nd Ed., pp. 196–212, Oxford University Press, Oxford, UK
3. Calderwood, D. A., Yan, B., de Pereda, J. M., Alvarez, B. G., Fujioka, Y., Liddington, R. C., and Ginsberg, M. H. (2002) *J. Biol. Chem.* **277,** 21749–21758
4. Calderwood, D. A., Huttenlocher, A., Kiosses, W. B., Rose, D. M., Woodside, D. G., Schwartz, M. A., and Ginsberg, M. H. (2001) *Nat. Cell Biol.* **3,** 1060–1068
5. Otey, C. A., Vasquez, G. B., Burridge, K., and Erickson, B. W. (1993) *J. Biol. Chem.* **268,** 21193–21197
6. Rajfur, Z., Roy, P., Otey, C. A., Romer, L., and Jacobson, K. (2002) *Nat. Cell Biol.* **4,** 286–293
7. Calderwood, D. A., Shattil, S. J., and Ginsberg, M. H. (2000) *J. Biol. Chem.* **275,** 22607–22610
8. Giancotti, F. G., and Ruoslahti, E. (1999) *Science* **285,** 1028–1032
9. Schoenwaelder, S. M., and Burridge, K. (1999) *Curr. Opin. Cell Biol.* **11,** 274–286
10. O'Toole, T. E., Katagiri, Y., Faull, R. J., Peter, K., Tamura, R., Quaranta, V., Loftus, J. C., Shattil, S. J., and Ginsberg, M. H. (1994) *J. Cell Biol.* **124,** 1047–1059
11. Nuckolls, G. H., Romer, L. H., and Burridge, K. (1992) *J. Cell Sci.* **102,** 753–762
12. Bolton, S. J., Barry, S. T., Mosley, H., Patel, B., Jockusch, B. M., Wilkinson, J. M., and Critchley, D. R. (1997) *Cell Motil. Cytoskelet.* **36,** 363–376
13. Albiges-Rizo, C., Frachet, P., and Block, M. R. (1995) *J. Cell Sci.* **108,**

3317–3329
14. Priddle, H., Hemmings, L., Monkley, S., Woods, A., Patel, B., Sutton, D., Dunn, G. A., Zicha, D., and Critchley, D. R. (1998) *J. Cell Biol.* **142,** 1121–1133
15. Monkley, S. J., Pritchard, C. A., and Critchley, D. R. (2001) *Biochem. Biophys. Res. Commun.* **286,** 880–885
16. Monkley, S. J., Zho, X.-H., Kinston, S. J., Giblett, S. M., Hemmings, L., Priddle, H., Brown, J. E., Pritchard, C. A., Critchley, D. R., and Fassler, R (2000) *Dev. Dynamics* **219,** 560–574
17. Brown, N. H., Gregory, S. L., Rickoll, W. L., Fessler, L. I., Prout, M., White, R. A., and Fristrom, J. W. (2002) *Dev. Cell* **3,** 569–579
18. Winkler, J., Lunsdorf, H., and Jockusch, B. M. (1997) *Eur. J. Biochem.* **243,** 430–436
19. Schmidt, J. M., Zhang, J., Lee, H.-S., Stromer, M. H., and Robson, R. M. (1999) *Arch. Biochem. Biophys.* **366,** 139–150
20. Rees, D. J. G., Ades, S. E., Singer, S. J., and Hynes, R. O. (1990) *Nature* **347,** 685–689
21. Hemmings, L., Rees, D. J. G., Ohanian, V., Bolton, S. J., Gilmore, A. P., Patel, N., Priddle, H., Trevithick, J. E., Hynes, R. O., and Critchley, D. R. (1996) *J. Cell Sci.* **109,** 2715–2726
22. Hamada, K., Shimizu, T., Matsui, T., Tsukita, S., Tsukita, S., and Hakoshima, T. (2000) *EMBO J.* **19,** 4449–4462
23. Calderwood, D. A., Zent, R., Grant, R., Rees, D. J. G., Hynes, R. O., and Ginsburg, M. H. (1999) *J. Biol. Chem.* **274,** 28071–28704
24. Pfaff, M., Liu, S., Erle, D. J., and Ginsberg, M. H. (1998) *J. Biol. Chem.* **273,** 6104–6109
25. Yan, B., Calderwood, D. A., Yaspan, B., and Ginsberg, M. H. (2001) *J. Biol. Chem.* **276,** 28164–28170
26. Borowsky, M. L., and Hynes, R. O. (1998) *J. Cell Biol.* **143,** 429–442
27. Muguruma, M., Nishimuta, S., Tomisaka, Y., Ito, T., and Matsumara, S. (1995) *J. Biochem.* (*Tokyo*) **117,** 1036–1042
28. McCann, R. O., and Craig, S. W. (1999) *Biochem. Biophys. Res. Commun.* **266,** 135–140
29. Xing, B., Jedsadayanmata, A., and Lam S. C. (2001) *J. Biol. Chem.* **276,** 44373–44378
30. Bass, M. D., Smith, B. J., Prigent, S. A., and Critchley, D. R. (1999) *Biochem. J.* **341,** 257–263
31. Garcia-Alvarez, B., de Pereda, J. M., Calderwood, D. A., Ulmer, T. S., Critchley, D. R., Campbell, I. D., Ginsberg, M. H., and Liddington, R. C. (2003) *Mol. Cell* **11,** 49–58
32. Di Paolo, G., Pellegrini, L., Letinic, K., Cestra, G., Zoncu, R., Voronov, S., Chang, S., Guo, J., Wenk, M. R., and De Camilli, P. (2002) *Nature* **420,** 85–89
33. Ling, K., Doughman, R. L., Firestone, A. J., Bunce, M. W., and Anderson R. A. (2002) *Nature* **420,** 89–93
34. Martel, V., Racaud-Sultan, C., Dupe, S., Marie, C., Paulhe, F., Galmiche, A., Block, M. R., and Albiges-Rizo, C. (2001) *J. Biol. Chem.* **276,** 21217–21227
35. Galbraith, C. G., Yamada, K. M., and Sheetz, M. P. (2002) *J. Cell Biol.* **159,** 695–705
36. Gilmore, A. P., and Burridge, K. (1996) *Nature* **381,** 531–535
37. Weekes, J., Barry, S. T., and Critchley, D. R., (1996) *Biochem. J.* **314,** 827–832
38. McNamee, H. P., Ingber, D. E., and Schwartz, M. A. (1993) *J. Cell Biol.* **121,** 673–678
39. Oude Weernink, P. A., Guo, Y., Zhang, C., Schmidt, M., von Eichel-Streiber, C., and Jakobs, K. H. (2000) *Eur. J. Biochem.* **267,** 5237–5246
40. Raucher, D., Stauffer, T., Chen, W., Shen, K., Guo, S., York, J. D., Sheetz, M. P., and Meyer, T. (2000) *Cell* **100,** 221–228
41. Marley, J. A., Lu, M., and Bracken, C. (2001) *J. Biomol. NMR* **20,** 71–75
42. Málnási-Csizmadia, A., Woolley, R. J., and Bagshaw, C. R. (2000) *Biochemistry* **39,** 16135–16146
43. Kaapa, A., Peter, K., and Ylanne, J. (1999) *Exp. Cell Res.* **250,** 524–534
44. Vinogradova, O., Velyvis, A., Velyviene, A., Hu, B., Haas, T. A., Plow, E. F., and Qin, J. (2002) *Cell* **110,** 587–597
45. Manes, S., Mira, E., Gomez-Mouton, C., Zhao, Z. J., Lacalle, R. A., and Martinez, A. C. (1999) *Mol. Cell. Biol.* **19,** 3125–3135
46. Niggli, V., Kaufmann, S., Goldmann, W. H., Weber, T. A., and Isenberg, G. (1994) *Eur. J. Biochem.* **224,** 951–957
47. Isenberg, G., and Goldmann., W. H. (1998) *FEBS Lett.* **426,** 165–170
48. Liddington, R. C., Bankston, L. A., and de Pereda, J. M. (2003) *Curr. Biol.* **13,** R94–R95